Influence of Dynamics on the Structure and NMR Chemical Shift of a Zeolite Precursor

Sailaja Krishnamurty,[†] Thomas Heine,[‡] and Annick Goursot*,[†]

LMCCCO UMR-CNRS 5618, ENSCM, 8 Rue de l'Ecole Normale, 34296, Montpellier Cédex 5, France, Department of Physical Chemistry, Université de Genève, 30 quai Ernest-Ansermet, CH-1211 Genève 4, Switzerland, and Inst. f. Physikalische Chemie, TU Dresden, D-01169 Dresden, Germany

Received: December 31, 2002; In Final Form: March 17, 2003

Density functional Born−Oppenheimer molecular dynamics (BOMD) is applied to study the evolution of geometry and ^{29}Si NMR chemical shifts of $Si(OH)_4$, which is the smallest zeolite precursor. Inclusion of water−precursor and water−water interactions is needed to obtain the NMR chemical shift in close agreement with experiment. The solvent influences the structural (SiOH angles) and electronic (polarization) parameters of the monomer. A linear correlation between the ⟨SiOH⟩ angles and the NMR chemical shifts is found. It is shown that the experimental NMR shift is indeed a sampling over a wide range of monomer conformations which varies over 50 ppm on the microscopic scale.

1. Introduction

Zeolites are crystalline microporous aluminosilicates used in a very wide variety of industrial applications.[1] They are synthesized under hydrothermal conditions, in the presence of various organic and inorganic additives.[2] The role of each component of the zeolitic synthetic gel in growing into one structure or another one is still a black box for experimentalists, despite an increasing number of experimental studies performed on the synthesis mixtures, using techniques such as nuclear magnetic resonance (NMR), transmission electron microscopy, and Raman, X-ray, and infrared scattering.[3,4]

These techniques revealed that the zeolite synthesis proceeds slowly via nucleation and that the chemical reactivity governs the solid growth. Among all the above methods, NMR is presently the best technique to study the initial stages of the synthesis in liquid−solid transformation, bringing in information at the molecular level.[5−11] Knight et al.[12] showed that, in the first few minutes, the NMR spectrum was characteristic essentially of the monomer silicate as the first precursor with a small amount of dimers and trimers, while larger units such as prisms or cubes appear only after several hours. However, though NMR provides useful information regarding the types of species present, the fundamental mechanism involved in the zeolite growing process remains unknown. Few theoretical studies have been devoted to these precursor species, reporting stable conformers[13−15] and chemical shifts,[15] but limited to their gas phase state.

In reality, the neglect of the presence of water, temperature effects, and evolution of the precursor as a function of time may be critical for a precise interpretation of the NMR spectra. We thus found it very interesting to explore the effects of the above-mentioned aspects using molecular dynamics (MD) on the simplest possible precursor species, that is, the monomer $Si(OH)_4$.

There have been few classical MD studies on the methanolic and ethanolic silica-based sol−gel solutions in the context of zeolite synthesis.[16,17] These methods are well suited to study geometries, but the electronic effects are completely neglected. Recent works with Car-Parinello MD[18,19] or combining MD and density functional theory (DFT)[20] have shown that averaging magnetic shieldings over MD trajectories is a practical approach to obtain good NMR chemical shifts.[18] In the present article we propose a density functional theory (DFT)-based Born Oppenheimer molecular dynamics (BOMD)[21] approach to evaluate ^{29}Si NMR chemical shifts of solvated zeolite precursors. The chemical shifts are calculated at room temperature with different cluster models varying from a plain $Si(OH)_4$ molecule to a solvated species with 4, 8, 10, and 14 water molecules. The parameters influencing the shielding constant, such as geometry, polarization, and simulation time, are studied carefully.

This study remains within the limitations of a classical description of the nuclear dynamics. The neglect of quantum effects for the hydrogen nuclei may induce some error in the ^{29}Si NMR shielding, although the spatial uncertainty of these hydrogens, Si second neighbors, is certainly negligible with respect to that reported for ^{13}C NMR shieldings in hydrocarbons.[22]

2. Computational Details

All calculations in this study employed DFT in the generalized gradient approximation of Perdew, Burke, and Ernzerhof (PBE).[23] A DZVP basis[24] was used for the dynamics. Calculations were performed using the deMon 2001[25] computer code with the following details: auxiliary basis functions were created automatically at the A2* level for Si (thus, including g-functions) and at the A2 level for other atoms.[25] The exchange correlation contributions were included using the fitted density. NMR calculations were performed using the IGLO method and zero-order DF perturbation theory, as implemented in the deMon-NMR package.[26] Molecular orbitals have been calculated using the IGLO-III basis set,[27] together with A2* auxiliaries, and transformed to localized MOs by employing the procedure of

[†] LMCCCO UMR-CNRS 5618, ENSCM. E-mail addresses: sailaja@palladium.enscm.fr, goursot@rhodium.enscm.fr.

[‡] Université de Genève and TU Dresden. E-mail: thomas.heine@chemie.tu-dresden.de.

10.1021/jp022686i CCC: $25.00
Published on Web 05/24/2003

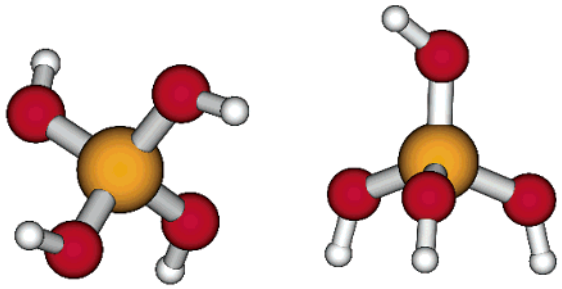

Figure 1. Optimized structures of the two $Si(OH)_4$ conformers **a** and **b**.

TABLE 1: Geometrical Parameters and $\delta(^{29}Si)$ of Two Local Minima of $Si(OH)_4$[a]

	a	b
E_{rel}	0.0	4.5
$\delta(^{29}Si)$	65.2	67.3
⟨SiOH⟩	114.2 ± 0.1	116.2 ± 0.4
⟨SiO⟩	1.66	1.66
exp $\delta(^{29}Si)$	71.3	

[a] The relative energy (E_{rel}) is given in kcal/mol, bond lengths are in Å, and angles are in deg (geometrical average). $\delta(^{29}Si)$ values are reported with respect to TMS in ppm, which has an absolute ^{29}Si magnetic shielding constant of 330.3 ppm at the same computational level and at the experimental geometry.[29]

Pipek and Mezey.[28] The NMR chemical shifts, $\delta(^{29}Si)$, were calculated with respect to that of tetramethylsilane (TMS) at its experimental geometry.[29] BOMD was implemented into the deMon 2001 code using the velocity-Verlet algorithm.[30] Coupling to an external heat reservoir was realized using the Berendsen thermostat.[31] If not specified otherwise, the dynamics was simulated at 300 K, using a time step of 0.03 fs. Trajectories were equilibrated to reach a stable total energy. Total simulation times, that is, the sum of trajectory times after equilibration, were 1.0−2.5 ps.

The evolution of the $Si(OH)_4$ conformations will be analyzed using the parameter ⟨SiOH⟩ , that is, the geometrical average of the four SiOH angles. On the other hand, we will compare the experimental $\delta(^{29}Si)$ with a ^{29}Si chemical shift calculated as the time-averaged value over the total simulation time. The corresponding time-averaged ⟨SiOH⟩ angle will then be used as a variable defining $Si(OH)_4$ at the microscopic scale.

3. Results and Discussion

(a) Static Investigations. Two local minima of $Si(OH)_4$ have been located using a full geometry optimization at the PBE/DZVP level. The most stable structure (conformer **a**) as shown in Figure 1 has four internal hydrogen bonds, while the 4.5 kcal/mol less stable conformer (conformer **b**) has larger SiOH angles and O−H bonds pointing to the outsides of the molecule. Thus, the geometry of conformer **b** corresponds more to the solvated molecule and has, indeed, a chemical shift 2 ppm closer to the experimental value for the monomer (71.3 ppm). The geometrical, energetic, and $\delta(^{29}Si)$ parameters obtained for the two conformers are given in Table 1. In contrast to the case of a simplified static model, the experimental chemical shift is an average over a few micro- to milliseconds and thus has contributions from many conformations which do not necessarily correspond to local minima. One of the possible ways to take into account the above factors is a DF-MD study and averaging the NMR chemical shift calculated at different time steps. The following sections discuss the results obtained from such studies in the presence and absence of water molecules around the monomer.

(b) Dynamic Investigations. Results from the MD simulations for gas-phase $Si(OH)_4$ as well as for several solvated models of $Si(OH)_4$ are summarized in Table 2 and discussed below.

(i) MD of Gas-Phase $Si(OH)_4$. $Si(OH)_4$ in the gas phase has been studied in three different ways: (i) running multiple trajectories of 0.5 ps simulation time after equilibration, starting from different structures, (ii) running one single trajectory of 2.5 ps, and, finally, (iii) checking the temperature effect by running multiple trajectories of 0.5 ps at a higher temperature (600 K). Before discussing the results, we first have to check the validity of the multiple trajectory approach by comparing (i) and (ii). The averaged values of the two approaches differ by only 0.3 ppm. This is beyond the numerical accuracy of the applied method and within the statistical errors. The difference between the maximum and minimum potential energies over the full trajectories is 10% larger for the long trajectory, which can be rationalized by the three times longer overall simulation time. However, as seen from Figure 2a, the range of ⟨SiOH⟩ values is larger for the multiple trajectories (103−127°) than for the long unique simulation (105−125°) due to the sampling of more conformations. The advantage of running several shorter trajectories instead of a single long one may become a necessity for larger systems: this way the simulation can be easily parallelized.

The first very striking result is the microscopic scale of the ^{29}Si chemical shift, ($\Delta\delta$), varying from 42 to 90 ppm and, thus, giving a range of almost 50 ppm. This is even more surprising when looking at the experimental scale of the $\delta(^{29}Si)$ for the zeolite precursors, which is less than 30 ppm with respect to the case of the monomer.

The second important result is the linear correlation ($r \geq 0.96$) between the ⟨SiOH⟩ angle of a given structure and its $\delta(^{29}Si)$. A scatter plot of this correlation is given in Figure 2b. Discussing the interrelation of these two observations, one can state that $Si(OH)_4$ in a gas-phase simulation is experiencing a very large spectrum of conformations, ever larger than the one a SiO_4 unit can have in any solid zeolite framework. The high flexibility of this molecule is an anticipated illustration of the high flexibility of the zeolite structures, in particular when they are hydrated or when they incorporate other elements than Si. This reference to zeolite structures is indeed supported by the ⟨SiOH⟩−$\delta(^{29}Si)$ linear correlation, which must be related with the ⟨SiOSi⟩−$\delta(^{29}Si)$ linear relationship reported for zeolites, in both experimental and theoretical studies.[32,33]

Studying the monomer at higher temperature (600 K) has little influence on the time-averaged values. However, as expected, the range of variation of ⟨SiOH⟩ (Δ⟨SiOH⟩) and that of the potential energy, E_{pot}, are much larger than those at 300 K (see Table 2). Moreover, the analysis of the trajectories shows that the conformer **b** population represents about 1.6−1.8%, which indeed corresponds to the expected Boltzmann population at that temperature.

All parameters calculated during the simulation are smooth functions in time, and the calculated $\delta(^{29}Si)$ values clearly follow the ⟨SiOH⟩ angles, as can be seen in Figure 3a. The relationship between the $\delta(^{29}Si)$ and the E_{pot} is not so straightforward.

Finally, the gas-phase MD results are little different from the static results of conformer **a**, which can be rationalized by the similar time-averaged ⟨SiOH⟩ angle of the trajectory and of the

TABLE 2: Time-Averaged Chemical Shifts and Angles Obtained from the Simulations

no. of H_2O	δ^{29}Si (ppm)	$\Delta\delta$ (ppm)	$\langle$SiOH$\rangle$ (deg)	$\Delta(\langle$SiOH$\rangle)$ (deg)	R	ΔE_{pot} (kcal/mol)	simulation time (au)
0[a]	66.0	48.0	114.8	22.0	0.96	10.7	32
0[b]	66.3	37.0	114.6	17.0	0.96	11.3	95
0[c]	65.9	71.0	114.6	33.0	0.97	22.6	32
4	66.8	36.0	114.8	18.0	0.97	18.8	32
4[d]	66.0	34.0			0.97	15.7	
8	69.7	55.0	116.2	21.0	0.98	39.9	32
8[d]	67.9	53.0			0.97	16.3	
10	69.5	34.0	115.8	17.0	0.98	25.0	20
10[d]	67.3	32.0			0.98	16.1	
14	69.4	17.3	115.8	9.8	0.95	25.1	20

[a] Multiple trajectories (300 K). [b] Long single trajectory (300 K). [c] Multiple trajectories (600 K). [d] NMR calculation removing the water shell.

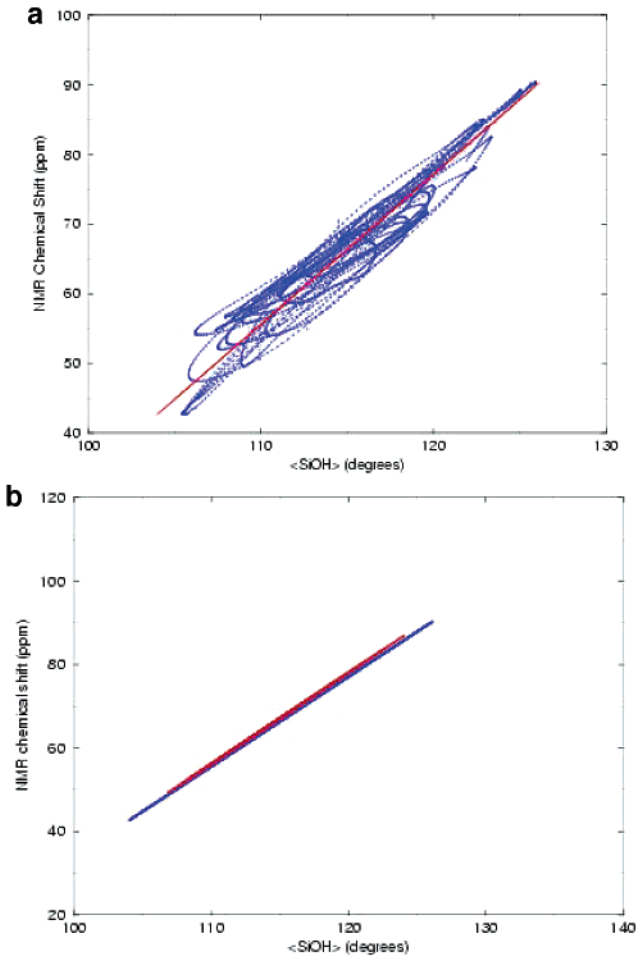

Figure 2. (a) Scatter plot of the geometrical average $\langle$SiOH$\rangle$ angle for $Si(OH)_4$ against the calculated $\delta(^{29}Si)$ obtained from multiple trajectories. The correlation is indicated by the red straight line. (b) Comparison between the correlations obtained with multiple trajectories (blue line) and one longer single trajectory (red line).

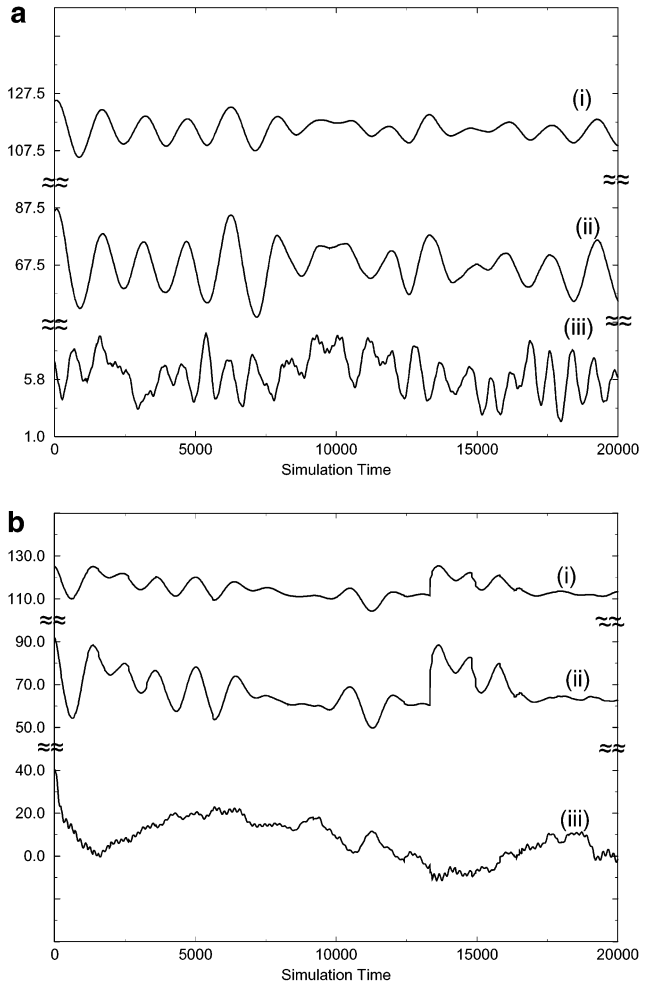

Figure 3. (a) $\langle$SiOH$\rangle$ angles (deg) (i), $\delta(^{29}Si)$ (ppm) (ii), and relative E_{pot} (kcal/mol) (iii) of $Si(OH)_4$ as a function of simulation time (au). (b) $\langle$SiOH$\rangle$ angles (deg) (i), $\delta(^{29}Si)$ (ppm) (ii), and relative E_{pot} (kcal/mol) (iii) of $Si(OH)_4$ with eight water molecules as a function of simulation time (au).

conformer. The difference of chemical shift with respect to experiment is about 5 ppm, which is far too large to assign precursor species to experimental shifts. In fact, theoretical predictions of δ^{29}Si in $Si(OR)_4$ compounds have reached an accuracy of 1−2 ppm,[33,34] in contrast to the case of silane compounds.[35] In the following section, the influence of the solvent will be analyzed.

(ii) MD of Solvated Models. To explore the role of the solvent, models of a monomer surrounded by water molecules have been created. The amount of water molecules is successively increased from 4, that is, having one water molecule per hydroxy group to allow a hydrogen bond, to 8, 10, and 14. The interactions of the water molecules among themselves increase with their number. The hydrogen bonds between the monomer and surrounding water and between water molecules themselves are dynamically formed and broken.

The models studied here can clearly be separated: the smallest model with only four water molecules, as taken by Moravetski et al.,[15] is giving very similar results to those for the gas phase monomer, only the range of potential energy is increasing. The time-averaged $\langle$Si−O−H$\rangle$ angle is only 0.2° larger than that in the gas phase, and thus the chemical shift is little different. The electronic influence of the four water molecules on the chemical shift, which is basically polarization, is on average 0.8 ppm and less than that expected experimen-

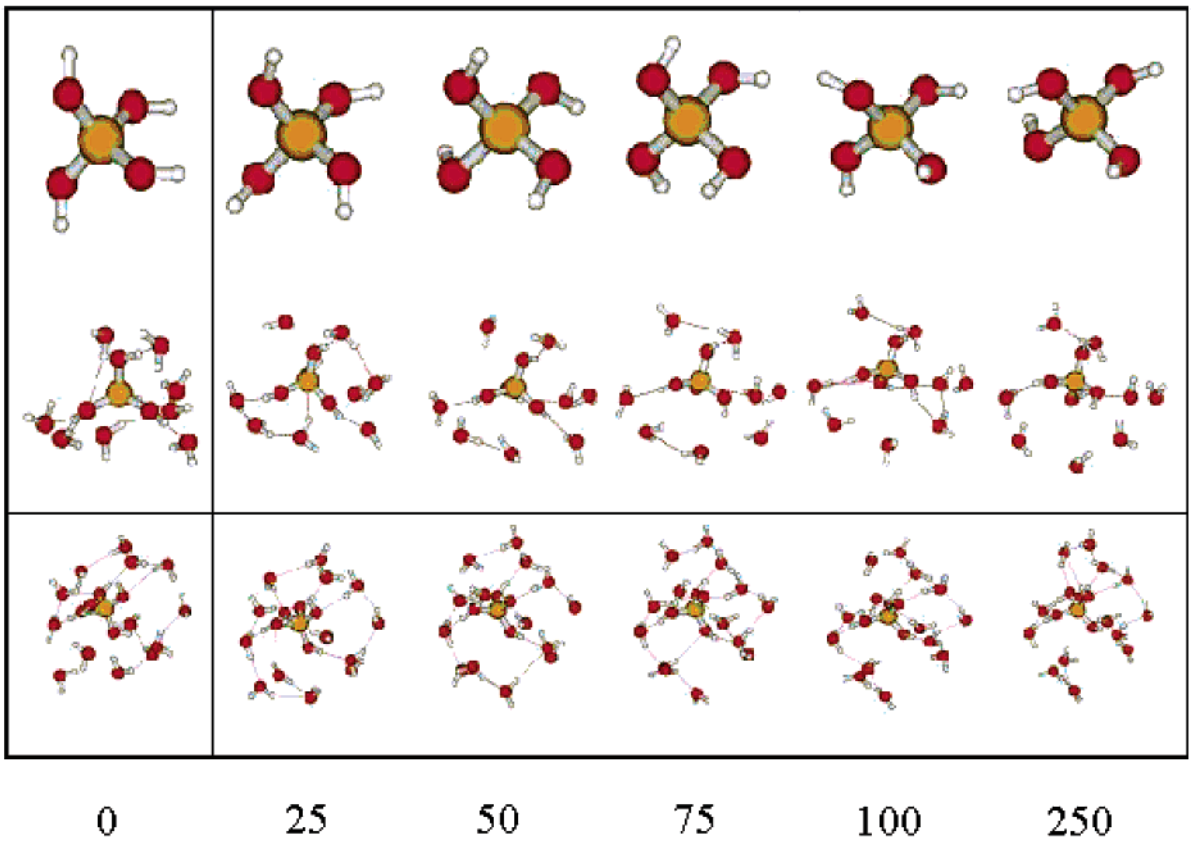

Figure 4. Snapshots from MD trajectories of $Si(OH)_4$ and $Si(OH)_4$ with 8 water molecules and $Si(OH)_4$ with 14 molecules (time in au).

tally. In summary, this small model is not adequate to simulate a solution, and it is qualitatively different from the second group of solvated models.

Models with 8 to 14 water molecules around the monomer agree qualitatively in their results. Comparison of parts a and b of Figure 3 shows that the presence of the water shell (here eight water molecules) is damping the oscillations of all functions in time.

As can be seen from Figure 4, these models have a complete shell of water molecules, which form a hydrogen bonded network. Averaged results are different from those for the gas phase and the small model with four water molecules: the time-averaged ⟨Si−O−H⟩ angle is 1−1.5° larger, and the chemical shift is closer to that of the experiment. For the models with 8−14 water molecules, the difference is still 1.5 ppm. Although this quantity should approach more the experimental value with increasing number of water molecules, this difference is within the methodological precision of the applied method.

Again, the time-averaged ⟨Si−O−H⟩ angle and $\delta(^{29}Si)$ are in linear correlation, and the chemical shift has a microscopic range of about 50 ppm, as can be seen in Table 2. The Si−O bond lengths are slightly larger by 0.02 Å than those in the gas phase, and the range of potential energy during the simulations is larger. There is only a weak correlation between $\delta(^{29}Si)$ and the Si−OH bond lengths because their variations during the simulations are very small, in contrast to the ⟨Si−O−H⟩ angle behavior.

The simulations allow us to quantify the contributions to the chemical shift arising from the solvent: running NMR calculations of the bare monomer, that is, by removing the water molecules from the monomer, gives the structural influence of the solvent, when comparing this chemical shift with the gas phase moiety. The structural influence can be quantified to be roughly 2 ppm toward experiment. The remaining 2 ppm can be assigned to the polarization of $Si(OH)_4$ by the water shell. Indeed, the water shell alone (without $Si(OH)_4$) does not create a shielding at the silicon site, as was confirmed by a NICS (nuclear independent chemical shift) calculation.[36] Thus, the presence of water in the quantum NMR calculation is essential for an accurate simulation of chemical shifts in solution.

4. Conclusions

This study has led to several useful results which will be beneficial for studies of larger zeolite precursors, presently in progress. From a technical point of view, our results have shown that average chemical shifts can be evaluated with short simulation times of about 2 ps, which is approximately a million times shorter than the time scale of an NMR measurement. In addition, the adequate periodicity for NMR snapshots has been established from comparisons of the average chemical shift and the standard deviation between evaluations at every 0.25, 0.50, 1, 1.5, and 2 fs. It was found that, at 1.5 fs, the results were affected by only 0.2 ppm, but that a further increase leads to a too large standard deviation.

More generally, this work allows us to infer that BOMD is the adequate method to study the evolution of zeolite precursors in the gel solution, comparing the average $\delta(^{29}Si)$ obtained from the simulations with experimental values. Indeed, ^{29}Si NMR spectra provide real fingerprints of the various species present in the gel solution, with the advantage of a very strong response to the chemical environment. BOMD integrates all the effects of this environment in time, especially the geometrical (hydrogen bonds) and polarization effects of the first neighbor solvent molecules. We think that this methodology can help to get insight into (i) the various precursor species recognized through their NMR spectra, (ii) the mechanism of zeolite growing from one species to a larger one, and (iii) the prominent role of cations and all other components of the gel solution in this mechanism.

Acknowledgment. S.K. acknowledges the Ministry of external affairs, France, and CNRS for fellowships. This work has been performed in the framework of the indo-french IFCPAR research project 2605-2. COST chemistry is acknowledged for funding short term scientific missions of S.K. and T.H. The authors acknowledge Peter Burger for providing computational facilities. Part of the calculations were carried out in the CINES computing center, Montpellier.

References and Notes

(1) Baerlocher, C. H.; Meier, W. M.; Olson, D. H. *Atlas of Zeolite Framework Types*, 5th ed.; Elsevier Science: Amsterdam, 2001.

(2) Breck, D. W. *Zeolite Molecular Sieves: Structure, Chemistry and Use*; Wiley Science: New York, 1974.

(3) Yang, S.; Vlessidis, A. G.; Evmiridis, N. P. *Ind. Eng. Chem. Res*. **1997**, *36*, 1622.

(4) Gilson, J. P. In *Zeolite Microporous Solids: Synthesis, Structure and Reactivity*; Derouane, E. G., Lemos, F., Naccache, C., Ribeiro, F. R., Eds.; Kluwer Academic Publishers: Amsterdam, 1992; p 19.

(5) Schoeman, B. J. *Zeolites* **1997**, *18*, 97.

(6) Engelhardt, G.; Michel, D. ^{29}Si NMR of Silicate Solutions. *High resolution solid-state NMR of silicates and zeolites*; John Wiley and Sons: 1987; Chapter 4, p 75.

(7) Gougeon, R.; Delmotte, L.; Le Nouen, D.; Gabelica, Z. *Microporous Mesoporous Mater*. **1998**, *26*, 143.

(8) Kirschhock, C. E. A.; Ravishanker, R.; Verspeurt, F.; Grobet, P. J.; Jacobs, P. A.; Martens, J. A. *J. Phys. Chem. B* **1999**, *103*, 4965.

(9) Mortlock, R. F.; Bell, A. T.; Radke, C. J. *J. Phys. Chem.* **1991**, *95*, 7847.

(10) Mortlock, R. F.; Bell, A. T.; Radke, C. J. *J. Phys. Chem.* **1991**, *95*, 372.

(11) Burkett, S. L.; Davis, M. E. *J. Phys. Chem.* **1994**, *98*, 4647.

(12) Harris, R. K.; Knight, C. T. G. *J. Chem. Soc., Faraday. Trans.* **1983**, *2*, 1525.

(13) Pereira, J. C. G.; Catlow, C. R. A.; Price, G. D. *J. Phys. Chem. A* **1999**, *103*, 3252.

(14) Pereira, J. C. G.; Catlow, C. R. A.; Price, G. D. *J. Phys. Chem. A* **1999**, *103*, 3268.

(15) Moravetski, V.; Hill, J. R.; Eichler, U.; Cheetam, A. K.; Sauer, J. *J. Am. Chem. Soc*. **1996**, *118*, 13015.

(16) Pereira, J. C. G.; Catlow, C. R. A.; Price, G. D. *J. Phys. Chem. A* **2001**, *105*, 1909.

(17) Pereira, J. C. G.; Catlow, C. R. A.; Price, G. D. *J. Phys. Chem. A* **2002**, *106*, 130.

(18) Bühl, M.; Parrinello, M. *Chem. Eur. J*. **2001**, *7*, 4487.

(19) Pfrommer, B. G.; Mauri, F.; Louie, S. G. *J. Am. Chem. Soc*. **2000**, *122*, 123.

(20) Malkin, V. G.; Malkina, O. L.; Steinebrunner, G.; Huber, H. *Chem. Eur. J*. **1996**, *2*, 452.

(21) Barnett, R. N.; Landman, U. *Phys. Rev. B* **1993**, *48*, 2081.

(22) Böhm, M. C.; Schulte, J.; Ramirez, R. *Int. J. Quantum Chem*. **2002**, *86*, 280.

(23) Perdew, J. P.; Burke, K.; Ernzerhof, M. *Phys. Rev. Lett.* **1996**, *77*, 3864.

(24) Godbout, N.; Salahub, D. R.; Andzelm, J.; Wimmer, E. *Can. J. Chem.* **1992**, *70*, 560.

(25) Köster, A. M.; Geudtner, G.; Goursot, A.; Heine, T.; Vela, A.; Salahub, D. R. *deMon*; Ottawa, Canada, 2001.

(26) Malkin, V. G.; Malkina, O. L.; Casida, M. E.; Salahub, D. R. *J. Am. Chem. Soc.* **1994**, *116*, 5898.

(27) Kutzelnigg, W.; Fleischer, U.; Schindler, M. In *NMR−Basic Principles and Progress*; Springer-Verlag: Heidelberg, 1990; Vol. 23, p 165.

(28) Pipek, J.; Mezey, P. G. *J. Chem. Phys.* **1989**, *90*, 4916.

(29) Beagley, B.; Monaghan, J. J.; Hewitt, T. G. *J. Mol. Struct*. **1971**, *8*, 401.

(30) Allen, M. P.; Tildesley, D. J. *Computer Simulation of Liquids*; Clarendon Press: Oxford, 1987.

(31) Berendsen, H. J. C.; Postma, J. P. M.; van Gunsteren, W. F.; DiNola, D.; Haak, J. R. *J. Chem. Phys.* **1984**, *81*, 3684.

(32) Fyfe, C. A.; Grondey, H.; Feng, Y.; Kokotailo, G. T. *J. Am. Chem. Soc.* **1990**, *112*, 8812.

(33) Valerio, G.; Goursot, A.; Vetrivel, R.; Malkina, O. L.; Malkin, V. G.; Salahub, D. R. *J. Am. Chem. Soc.* **1998**, *120*, 11426.

(34) Valerio, G.; Goursot, A. *J. Phys. Chem.* **1999**, *103*, 51.

(35) Heine, T.; Goursot, A.; Seifert, G.; Weber, J. *J. Phys. Chem. A* **2001**, *105*, 620.

(36) Schleyer, P. V.; Maerker, C.; Dransfeld, A.; Jiao, H.; van Eikema Hommes, J. R. *J. Am. Chem. Soc*. **1996**, *118*, 6317.